Eur Biophys J (1987) 15:197–210

European Biophysics Journal

A molecular dynamics simulation of crystalline α-cyclodextrin hexahydrate

J. E. H. Koehler [1], W. Saenger [1] *, and W. F. van Gunsteren [2]

[1] Institut für Kristallographie, Freie Universität Berlin, Takustrasse 6, D-1000 Berlin 33, Germany
[2] Department of Physical Chemistry, The University of Groningen, Nijenborgh 16, NL-9747 AG Groningen, The Netherlands

Received September 22, 1986/Accepted in revised form April 30, 1987

Abstract. The structure of crystalline α-cyclodextrin (α-CD) hexahydrate, form I ($C_{36}H_{60}O_{30} \cdot 6H_2O$, space group $P2_12_12_1$) is experimentally so well determined by X-ray and by neutron diffraction analyses that the positions of all the hydrogen atoms are available. This provides an opportunity for testing an empirical force field that is currently used in simulations of protein and nucleic acid structures by performing molecular dynamics studies employing the GROMOS program package on a system of 4 unit cells containing 16 α-CD molecules and 96 water molecules.

A detailed comparison of the simulated and experimentally determined crystal structures shows that the experimental positions of the α-CD atoms are reproduced within 0.025 nm, well within the overall experimental accuracy of 0.036 nm; that the water molecules are on average within 0.072 nm from their experimental sites, with two thirds reproduced within experimental accuracy by the calculations; that high correlation is produced between the occurrence of simulated and experimentally observed hydrogen bonds.

The good agreement between simulated and experimental results suggests that the tested force field is reliable.

Key words: α-cyclodextrin hexahydrate, molecular dynamics simulation, empirical force field, hydrogen bonds

Introduction

Cyclodextrins (CD) are a family of cyclically closed, torus shaped oligosaccharides consisting of six (α), seven (β), and eight (γ) glucose units covalently linked by α(1–4) bonds. Their most remarkable properties, the inclusion of guest (substrate) molecules in the annular cavities with 5 to 7 Å diameter, have been studied in great detail with spectroscopic and crystallographic methods (Cramer et al. 1967; Saenger 1980). The guest molecules can vary from hydrophilic to hydrophobic in character, the only condition for inclusion being that they are small enough to fit spatially into the cavity. Owing to their microheterogeneous properties brought about by the hydrophobic cavity and the hydrophilic rims lined with O–H groups, the CD's exert diverse catalytic activities which made them good enzyme models (Cramer et al. 1967; Saenger 1980).

The CD's can be crystallized as inclusion complexes or, from pure water, as hydrates. In these, extended hydrogen bonding networks are formed because there are a large number of O–H groups from water molecules and from O2, O3, and O6 hydroxyls (Hingerty et al. 1984). The α-CD · $6H_2O$ form I complex has four water molecules outside and two inside the CD ring and represents the "empty" α-CD occurring in aqueous solution without a guest molecule added. Its structure has been determined from X-ray diffraction (Manor and Saenger 1974) and from neutron diffraction data (Klar et al. 1980). Figure 1 shows a schematic picture of α-CD as obtained from the X-ray diffraction work with the two water molecules included in its cavity.

In the α-CD ring, glucose unit 5 is rotated to diminish the cavity so that the enclosed water molecules are held tightly. The interglucose, intramolecular O2 ... O3 hydrogen bonds are all formed except to this glucose and this conformation also allows hydrogen bonding of two O6 hydroxyls to one of the enclosed water molecules. If complex formation occurs, the included water molecules are released, the distortion vanishes, the α-CD adopts a "round" shape with all O2 ... O3 hydrogen bonds formed and the guest molecule is enclosed (Saenger 1980). There is another crystal structure of α-CD · $6H_2O$, called form II, where only one water molecule and the O6 hydroxyl of an adjacent α-CD are inside the cavity (Lindner

* To whom offprint requests should be sent

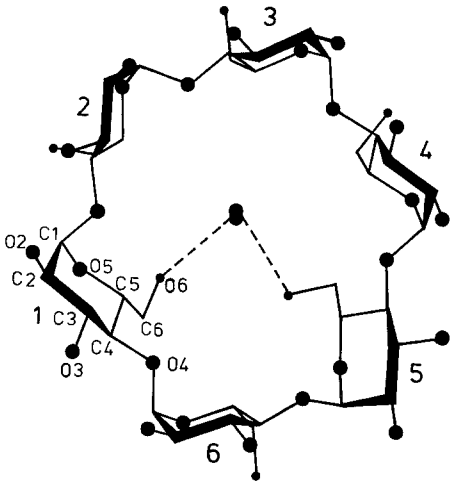

Fig. 1. Schematic structure of α-cyclodextrin molecule as derived from X-ray and neutron diffraction studies (Manor and Saenger 1974; Klar et al. 1980). Atom names in the first glucose unit and the numbering of glucose units are shown. The two included water molecules are shown with their hydrogen bonds to the O6 hydroxyl groups of glucose unit 1 and 5

and Saenger 1982), and the α-CD adopts a shape as in form I crystals. A third crystal structure exists, α-CD · $7.57\,H_2O$, called form III, with five waters outside and 2.57 water molecules included in the cavity. They are distributed over 4 sites, each with about 0.64 occupancy, and the α-CD occurs in the "round" conformation commonly observed in complexes of α-CD with guest molecules (Chacko and Saenger 1981).

Because of the interesting structural and catalytic properties of the cyclodextrins we decided to study α-CD using the computer simulation method of molecular dynamics (MD). When performing MD, the equations of motion of the individual atoms of the molecules are solved numerically. This yields atomic trajectories from which various structural and dynamic properties can be obtained. Some of these calculated properties can subsequently be compared to the experimentally obtained ones. This comparison may serve as a test of the molecular model and force field that is used in the simulation.

This paper describes the results of a 15 ps MD simulation of a molecular system as found in the crystal structure of α-CD · $6\,H_2O$ form I at 293 K. It serves two purposes; *(i)* because of the good structure data obtained from the high resolution X-ray and neutron diffraction studies, this system will make an excellent test case for the molecular model and force field that is applied; *(ii)* the atomic trajectories of the MD simulation may be used to analyse dynamic properties that are inaccessible to experimental probes.

This study differs from similar MD simulation studies of crystalline proteins (van Gunsteren et al. 1983; Krüger et al. 1985; Berendsen et al. 1986) because reliable atomic coordinates of hydrogen atoms of both solute and water molecules were obtained from neutron diffraction studies. This yields the opportunity of testing the quality with which the solute–water interactions are reproduced in the force field that is used. Solute–water interactions have also been studied in other crystalline systems like the dCpG/proflavin complex (Mezei et al. 1983; Kim and Clementi 1985) and vitamin B_{12} (Vovelle et al. 1985) using the Monte Carlo simulation method. However, in these studies all solute atoms were kept fixed and only the water molecules were allowed to move, whereas in our α-CD · $6\,H_2O$ simulation all 1,632 solute and water atoms were free to move.

Model and computational procedure

The experimental data referred to in this paper for α-CD · $6\,H_2O$, form I, haven been taken from the neutron diffraction study (Klar et al. 1980). The $C_{36}H_{60}O_{30} \cdot 6\,H_2O$ complex crystallises at room temperature in the orthorhombic space group $P2_12_12_1$ with unit cell dimensions $a = 1.4858$ nm, $b = 3.4038$ nm, $c = 0.9529$ nm. There are four molecules per unit cell ($Z = 4$). The structure was refined to an R-value of 12.0% for 2,808 neutron data (8.8% for 1,963 "observed" data) and to 3.7% for 4,268 X-ray data (Klar et al. 1980; Manor and Saenger 1974). The hydroxyl O61 position was found to be twofold disordered, with the O61A site 92% occupied and the O61B site 8%, all other atom sites are fully occupied. The hydrogen-atom HO61B attached to the low occupancy site could not be located from the neutron data, but the hydrogen atom attached to the high occupancy site, HO61A, was clearly found. The O61A site coordinates were used in the MD simulation. The two water molecule sites within the α-CD torus (see Fig. 1) are denoted by OWA and OWB, the others by OW1 to OW4.

The molecular dynamics (MD) simulation of α-CD · $6\,H_2O$, form I, at 293 K was carried out using the GROMOS (Groningen Molecular Simulation) computer program package. The molecular model that is used treats all atoms explicitly, except for the hydrogen atoms that are bound to carbon atoms. These are incorporated into the latter forming "united atoms" so that each α-CD molecule consists of 84 "atoms". The seven different atom types occurring in the α-CD · $6\,H_2O$ system are listed in Table 1. Because the cut-off radius $R_c = 0.8$ nm must be smaller than half of the box length, the unit cell was translationally doubled in the a and c directions. Therefore, the computational box that is simulated consists of 4 unit cells each containing 4 α-CD molecules and 24 water molecules, with dimensions 2a, b, 2c and with a total of

$N_{at} = 1{,}632$ atoms. The potential energy function describing the interactions between the atoms consists of five different terms (van Gunsteren and Berendsen 1985; Åqvist et al. 1985)

$$V(r_1, r_2, \ldots, r_{N_{at}}) \quad (1)$$

$$= \sum_{l=1}^{N_b} 1/2\, K_{b_l}(b_l - b_{0_l})^2 + \sum_{l=1}^{N_\theta} 1/2\, K_{\theta_l}(\theta_l - \theta_{0_l})^2$$

$$+ \sum_{l=1}^{N_b} 1/2\, K_{\xi_l}(\xi_l - \xi_{0_l})^2 + \sum_{l=1}^{N_\varphi} K_{\varphi_l}(1 + \cos(n_l \varphi_l - \delta_l))$$

$$+ \sum_{i<j}^{N_{at}} (C_{12}(i,j)/r_{ij}^{12} - C_6(i,j)/r_{ij}^6 + q_i q_j/(4\pi\varepsilon_0 \varepsilon_r r_{ij})).$$

The Cartesian position vectors of the N_{at} atoms in the computational box are denoted by $\boldsymbol{r}_1, \boldsymbol{r}_2, \ldots, \boldsymbol{r}_{N_{at}}$. In the first term the summation runs over all N_b covalent bonds l in the system. The current bond length of bond l is denoted by b_l and the force constants K_{b_l} and ideal bond lengths b_{0_l} are parameters of the energy function. The values of the parameters of the GROMOS force field are given in Table 2.

The summation in the second term runs over all N_θ bond angles l. The current bond angle is denoted by θ_l, and the parameters K_{θ_l} and θ_{0_l} are given in Table 2 for the various types of bond angles. The torsion angles are divided into two classes: torsion angles ξ, also called improper torsion angles, which keep certain atoms near planar or tetrahedral configurations, obeying a harmonic potential (third term), and torsion angles φ that may perform complete (360°) rotations, obeying a sinusoidal potential (fourth term). The definition of the improper torsion angles for the five tetrahedral carbon atoms in the glucose units are given in Table 2. In total, $N_\xi = 480$ in the third term of Eq. (1). The definition of the (proper) torsion angles, φ (fourth

Table 1. Force field parameters. Atom names in the glucose units are defined in Fig. 1. Atoms in water molecules are denoted by OW, HW1, HW2. The partial charges q_i are given in electronic units

Atom name	Partial charge q_i	Atom type	Characterization
C1	0.400	CS1	Sugar CH1-group
C2, C3	0.150		
C4, C5	0.160		
C6	0.150	CS2	Sugar CH2-group
O4, O5	−0.360	OS	Sugar oxygen
O2, O3, O6	−0.548	OA	Hydroxyl oxygen
H2, H3, H6	0.398	HA	Hydroxyl hydrogen
OW	−0.820	OW	Water oxygen
HW1, HW2	0.410	HW	Water hydrogen

Table 2. Force field parameters for bond lengths, angles, and (improper) torsion angles. Atom types are defined in Table 1, atom names in Fig. 1. The parameters are defined in Eq. (1). The value of δ is zero for all proper torsion angles. The units are in kcal and Å

Bond	K_b [kcal mol^{-1} Å^{-2}]	b_0 [Å]
CS–CS	600	1.52
CS–OS	600	1.435
CS–OA	600	1.43
OA–HA	750	1.00
OW–HW	–	1.00

Bond angle	K_θ [kcal mol^{-1} rad^{-2}]	θ_0 [degrees]
CS–CS–CS	60	109.5
CS–CS–OS, CS–CS–OA, OS–CS–OS	68	109.5
CS–OS–CS	80	109.5
CS–OA–HA	95	109.5
HW–OW–HW	–	109.5

Improper torsion angle	K_ξ [kcal mol^{-1} rad^{-2}]	ξ_0 [degrees]
C1–O5–O4–C2, C5–O5–C6–C4, C2–O2–C3–C1, C3–O3–C2–C4, C4–C3–O4–C5	80	35.264

Torsion angle	K_φ [kcal mol^{-1}]	n
C4–O4–C1–C2	0.9	3
O4–C1–C2–C3	1.4	3
O4–C1–C2–C3	0.1	2
O5–C1–C2–C3	0.1	2
O5–C1–C2–O2	0.5	2
O4–C1–C2–O2	0.5	2
C1–C2–O2–H2	0.3	3
C1–C2–C3–C4	1.4	3
C1–C2–C3–O3	0.1	2
O2–C2–C3–C4	0.1	2
O2–C2–C3–O3	0.5	2
C2–C3–O3–H3	0.3	3
C2–C3–C4–C5	1.4	3
C2–C3–C4–O4	0.1	3
O3–C3–C4–C5	0.1	3
O3–C3–C4–O4	0.5	3
C2–C1–O5–C5	0.9	3
C1–O5–C5–C4	0.9	3
C4–C5–C6–O6	1.4	3
C4–C5–C6–O6	0.1	2
O5–C5–C6–O6	0.5	2
C5–C6–O6–H6	0.3	3
C6–C5–C4–C3	1.4	3
O5–C5–C4–C3	0.1	2
C6–C5–C4–O4	0.1	2
O5–C5–C4–O4	0.5	2
C3–C4–O4–C1	0.9	3

Table 3. Force field parameters; van der Waals interactions. Atom types are defined in Table 1. The parameters are defined in Eq. (1). For each entry the upper value is to be taken for general non-bonded atom pairs, the lower value for third neighbour pairs

	General pairs (i,j) Third neighbours (i,j)									
Atom type	OA/OS	OW	HA/HW	CS1	CS2	OA/OS	OW	HA/HW	CS1	CS2
	10^9 C12 (i,j) [kJ mol^{-1} nm^{12}]					10^6 C6 (i,j) [kJ mol^{-1} nm^6]				
OA/OS	1 506	1 992	0	7 294	5 119	2 262	2 433	0	5 316	4 536
	1 506	1 992	0	1 665	2 297	2 262	2 433	0	2 566	3 269
OW		2 633	0	7 294	5 119		2 617	0	5 719	4 879
		2 633	0	1 665	2 297		2 617	0	2 760	3 516
HA/HW			0	0	0			0	0	0
			0	0	0			0	0	0
CS1				71 750	12 030				12 500	10 660
				3 736	5 156				2 912	3 709
CS2					35 330					9 098
					7 115					4 724

term) is also given in Table 2. We note that a few torsion angles occur twice with different multiplicities n, which makes it possible to model the rotational potential well more accurately, with $N_\varphi = 2\,592$. When calculating the nonbonded interactions in the fifth term of Eq. (1), atoms which are separated by one or two covalent bonds (1st and 2nd next neighbours), are excluded. However, for third neighbours this term will contribute to the overall rotational energy profile. Therefore, the van der Waals parameters for third neighbour atom pairs are different from those for a general atom pair (Table 3). The atomic partial charges are given in Table 1 for a dielectric constant $\varepsilon_r = 1$. When evaluating the summation in this last therm, a cut-off radius $R^c = 0.8$ nm is applied, beyond which no interactions are included. This value is chosen slightly smaller than half the value of the smallest edge of the computational box.

Since $R^c < 0.9529$ nm, an atom cannot interact simultaneously with another atom and its periodic image. Even with this value of R^c, the summation over the nonbonded interactions runs over typically 10^5 atom pairs. To reduce computing costs, the list of nonbonded atom pairs is kept constant over 10 MD time steps of $\Delta t = 2$ fs. The cut-off radius R^c is applied to centres of geometry of neutral atom groups and to the oxygen atoms of the water molecules, in order to avoid the breaking of the charge neutrality of a group or of a water molecule in case an atom–atom cut-off is applied. For the cyclodextrins these neutral atom groups are: (C4, O4, C1, O5, C5), (C2, O2, H2), (C3, O3, H3) and (C6, O6, H6).

As in previous simultaneous (van Gunsteren et al. 1983; Krüger et al. 1985; Berendsen et al. 1986; Åqvist et al. 1985) all bond lengths are kept rigid during the simulation by using the SHAKE method (Ryckaert et al. 1977; van Gunsteren and Berendsen 1977). This does not affect the properties of the system while saving a factor 3 in computing time (van Gunsteren and Karplus 1982; Berendsen and van Gunsteren 1984). The water molecules are modelled by a simple rigid three point charge (SPC) model (see Tables 1, 2, and 3), which adequately describes the properties of bulk water at room temperature (Berendsen et al. 1981).

Before starting the MD simulation the initial configuration was energy minimized in order to release possible strain. Initial velocities for the atoms were taken from a Maxwellian distribution at 293 K, independently for each of the molecules. The system was weakly coupled to a thermal bath of $T_0 = 293$ K, when integrating the equations of motion with time steps $\Delta t = 2$ fs. This was done by applying the algorithm with temperature relaxation time $\tau = 0.1$ ps. This value makes the temperature coupling weak enough to avoid any significant effect on the atomic properties of the system (Berendsen et al. 1984). Periodic boundary conditions corresponding to the crystal translational symmetry ($2a, b, 2c$) were applied.

The MD run covered a time span of 15 ps. After a few ps the total potential energy remained at a constant level and the root mean square positional difference between the actual structure and the initial structure also reached a constant value. Therefore, the equilibration period was chosen to be 5 ps. After the final 10 ps, coordinates were stored every 0.01 ps to be used for analysis. The molecules in the 16 asymmetric units moved independently. To sum up, statistical averaging was performed over the time period 5–15 ps and over the 16 asymmetric units. This average is denoted as $\langle M\,1\text{–}16;\ 5\text{–}15\,\text{ps}\rangle$.

Table 4. Root mean square positional differences and simulated fluctuations between various α-cyclodextrin structures. The experimental structure is denoted by X_{exp}. Averages over simulated structures are denoted by the symbol $\langle \ldots \rangle$, where M refers to one or more of the 16 molecules in the computational box and the averaged time span is given in picoseconds. The mean is over the 6 glucose units in α-cyclodextrin. The values are given in nm. Experimental rms fluctuations have been calculated using the formula $(3 \cdot B_{iso}/(8\pi^2))^{1/2}$, where the isotropic B-factor is denoted by B_{iso}. The ratios between the shortest and longest axes of the thermal motion ellipsoids are given

	$X_{exp}/\langle M1-16; 5-15\,ps\rangle$					$X_{exp}/\langle M1-16; 5-10\,ps\rangle$		$X_{exp}/\langle M1; 5-15\,ps\rangle$		$\langle M1; 5-15\,ps\rangle/\langle M5; 5-15\,ps\rangle$
	rms difference	Isotropic rms fluctuation		Anisotropic ratio between shortest and longest axes of thermal ellipsoids		Difference	Fluctuation	Difference	Fluctuation	Difference
	exp/MD	exp	MD	exp	MD	exp/MD	MD	exp/MD	MD	exp/MD
C1	0.020	0.031	0.036	0.73	0.64	0.021	0.036	0.027	0.038	0.024
C2	0.019	0.032	0.036	0.73	0.66	0.020	0.037	0.030	0.038	0.031
C3	0.011	0.030	0.035	0.81	0.72	0.013	0.035	0.013	0.036	0.024
C4	0.013	0.030	0.034	0.76	0.68	0.014	0.034	0.013	0.036	0.021
O4	0.016	0.031	0.036	0.73	0.67	0.017	0.036	0.015	0.038	0.020
C5	0.020	0.031	0.037	0.81	0.66	0.021	0.037	0.022	0.039	0.021
O5	0.021	0.032	0.039	0.76	0.61	0.022	0.039	0.027	0.041	0.024
O2	0.023	0.036	0.045	0.65	0.59	0.026	0.045	0.042	0.044	0.046
H2	0.054	0.044	0.081	–	–	0.060	0.081	0.100	0.066	0.101
O3	0.012	0.034	0.044	0.72	0.62	0.014	0.044	0.018	0.043	0.027
H3	0.029	0.043	0.065	–	–	0.033	0.068	0.042	0.056	0.040
C6	0.023	0.036	0.046	0.76	0.54	0.024	0.045	0.029	0.046	0.030
O6	0.020	0.038	0.053	0.69	0.54	0.020	0.050	0.026	0.053	0.033
H6	0.037	0.044	0.071	–	–	0.036	0.064	0.053	0.066	0.053
All atoms excl. H	0.018	0.033	0.040	0.74	0.63	0.020	0.040	0.025	0.041	0.028
All atoms	0.025	0.036	0.049	–	–	0.027	0.049	0.039	0.047	0.041

Results and discussion

α-CD structure and dynamics

The structure of α-CD · $6H_2O$ as derived from the MD simulation was obtained by averaging over the 16 molecules during the time period from 5 to 15 ps. This averaging yields the atomic root mean square positional fluctuations:

$$\mathrm{rms}_{\mathrm{pos.\,fluc.}} = \left(\sum_{\substack{i=1 \\ (x,y,z)}}^{N} \langle (x_i^{\mathrm{MD}} - \langle x_i^{\mathrm{MD}} \rangle)^2 \rangle / N \right)^{1/2}, \quad (2)$$

where the summation i runs over a specified set of N atoms and over the three Cartesian components. Averaging over corresponding atoms in different asymmetric units and over time is denoted by $\langle \ldots \rangle$.

The average structure is compared with the experimental one in terms of the root mean square difference of the atomic positions

$$\mathrm{rms}_{\mathrm{pos\ diff.}} = \left(\sum_{\substack{i=1 \\ (x,y,z)}}^{N} (x_i^{\mathrm{exp}} - \langle x_i^{\mathrm{MD}} \rangle)^2 / N \right)^{1/2}. \quad (3)$$

Both quantities are shown in Table 4. If not quoted otherwise, averaging means taking the root mean square average.

The coordinates of non-hydrogen atoms of the sugar differ from experiment by about 0.018 nm (lowest 0.011, highest 0.023 nm), whereas for the three hydroxyl hydrogen atoms the average is around 0.040 nm (0.029 to 0.054 nm). The overall averaged rms deviation for all atoms is 0.025 nm (column 1 in Table 4). Comparison of an arbitrarily chosen molecule, e.g. $M1$, with the experimental data leads to larger rms values with an overall average deviation of 0.039 nm for all atoms. The development of the geometry of different molecules during the MD simulation can be different, as is shown in the last column in Table 4, where $M1$ and $M5$ are compared to each other. The difference is of the same order of magnitude as the deviation of each of them from the experimental structure. Averaging over the 16 molecules in the computational box does improve the agreement with experiment significantly. Averaging over 5 ps instead of 10 ps does not significantly change the resulting deviations and fluctuations.

When comparing the structures of two molecules it is common practice to fit them as well as possible to each other. One may perform a translational fit by superimposing the centres of mass of both molecules and subsequently perform a least squares rotational fit around the shared centre of mass. When performing a

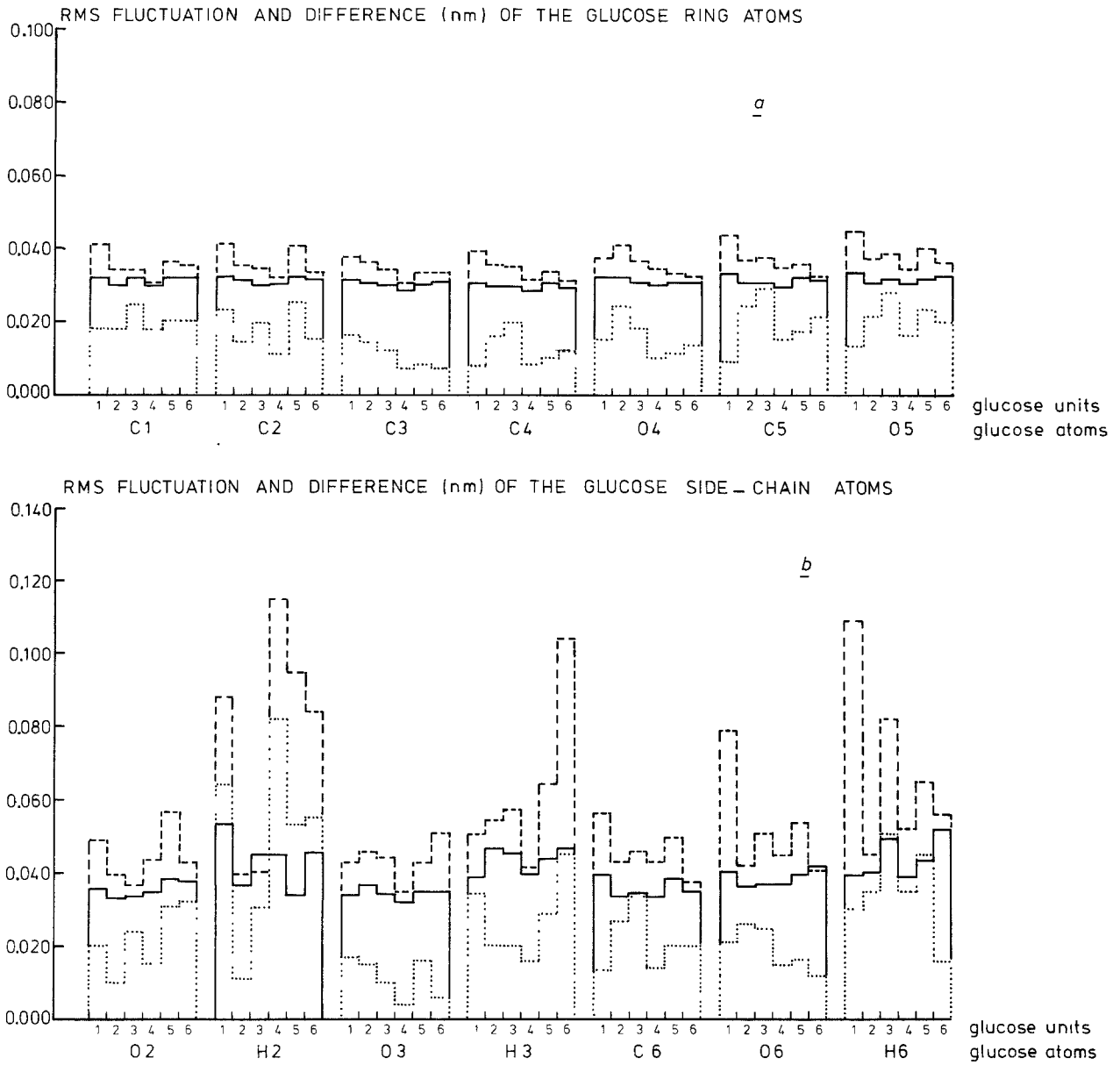

Fig. 2a and b. Rms positional fluctuations and differences (in nm) of main chain atoms (**a**) and side-chain atoms (**b**) in the 6 glucose unis. *Solid line:* fluctuation as derived from experimental isotropic *B*-factors; *dashed line:* fluctuation obtained from the MD stimulation $\langle M1-16;\ 5-15\,\text{ps}\rangle$; *dotted line:* difference between MD averaged structure and experimental structure

translational fit the agreement with the experimental structure improves marginally from 0.025 nm to 0.024 nm. When performing a rotational fit to the C3 carbon atom positions the agreement is 0.023 nm. Throughout this paper no fit procedures will be applied.

Crystallographic refinement techniques yield atomic *B*-factors which give an indication of atomic thermal vibrations in the crystal lattice. The isotropic *B*-factor is related to the atomic rms positional fluctuation as defined in Eq. (2) by

$$\text{rms}_{\text{pos. fluc.}} = (3\,B_{\text{iso}}/(8\,\pi^2))^{1/2}\,. \qquad (4)$$

The experimental and MD values for rms positional fluctuations are also listed in Table 4. The MD values are about 0.01 nm larger than the experimental ones, but the relative size for the various atoms is nicely reproduced in the simulation. The MD values are significantly larger than the crystallographic ones for atoms at the end of a covalent chain, like HO2, HO3, and HO6. This may partly be due to the finding that crystallographic refinement procedures tend to underestimate the *B*-factors of mobile side chain atoms (Kuriyan et al. 1986). The rms fluctuations of the individual α-CD atoms are shown in Fig. 2. The experimental fluctuations of the main chain atoms (solid

lines) are well reproduced by the simulation (dashed lines). For the eight side chain atoms HO21, HO24, HO25, HO26, HO36, O61, HO61 and HO63 the mobilities are much larger than reflected in the crystallographic temperature factors.

Figure 2 also shows that the deviation of the MD structure from the experimental one (dotted lines) is smaller than the experimental fluctuation as derived from Eq. (4) (solid lines). This means that the MD simulation reproduces the atomic positions in the crystal lattice within their experimentally determined accuracy.

From crystallographic data, anisotropic *B*-factors are available for non-hydrogen atoms (Klar et al. 1980; Manor and Saenger 1974). In Table 4 the ratio between the shortest and longest axes of the thermal motion ellipsoids (averaged over the glucose units) are given. For the individual atoms the experimental values range from 0.54 to 0.90 and the MD-values from 0.40 to 0.84. The simulation shows more anisotropy in the atomic motions and also a larger variation in anisotropy when comparing atoms in different glucose units. As with the isotropic *B*-factors, the anisotropic refinement procedures tend to underestimate the anisotropy of mobile atoms. This may be checked by applying the crystallographic anisotropic refinement procedure to the diffraction intensities as they can be directly calculated from the simulated trajectories of the system.

Another way to assess the experimental and the simulated structure is to compare the various bond angles and torsion angles (Table 5). All bond angles of the α-CD glucose ring and O–H groups have been well reproduced within a difference ranging from 0.9° to 5.6°, with the exception of the angle C2–O 2–HO2 (exp. 108.5°, MD 114.3°). The MD bond angle fluctuations range from 3.2° to 4.7°. The glucose ring torsion angles show a slightly larger flexibility; their MD fluctuations range from 5.6° to 6.7°. As to the differences between experiment and MD simulation, torsion angles around C4 (C2–C3–C4–C5 and C3–C4–C5–O5) are ~4.6° smaller in the MD simulation than in experiment, indicative of a general flattening at the glucosidic link atom.

The difference between MD and experimental glucosidic bond torsion angles are within 5° to 6° (Table 5). The largest deviation of 12.4° is observed for the angle C36–C46–O46–C15 (exp. 170.9°, MD 158.5°). The large experimental value for this angle reflects the twisted orientation of glucose unit 5 when compared to the other units, where C3–C4–O4–C1′ angles are 116.8° to 134.7°. We note that the relative variation of the values for the different glucose units is also observed in the simulation. The glucosidic bond torsion angles show slightly larger fluctuations (8°) than the ring torsion angles (6°).

Table 5. Bond- and torsion angles, their differences and fluctuations in α-cyclodextrin. The values averaged over the 6 glucose units for the experimental structure and for the MD structure (⟨*M*1–15; 5–15 ps⟩) are given (in degrees) in the first two columns. The third column gives the rms difference between the experimental and MD values. The last column contains the rms dynamical fluctuation of the angles as observed in the simulation

a) α-cyclodextrin bond-angles

	Bond angle		Difference	Fluctuation
	exp	MD	exp/MD	MD
C2–C1–O4	108.2	113.6	5.6	3.9
C1–O5–C5	114.3	114.2	0.9	3.4
C5–C6–O6	111.2	114.4	3.9	4.7
C2–O2–H2	108.5	114.3	13.1	4.3
C3–O3–H3	109.2	109.1	2.9	4.3
C6–O6–H6	107.9	109.4	4.2	4.4
All			4.1	4.0

b) α-cyclodextrin glucose ring torsion angles

	Torsion angle		Difference	Fluctuation
	exp	MD	exp/MD	MD
C1–C2–C3–C4	−52.4	−52.1	1.9	6.6
O5–C1–C2–C3	+57.1	+56.7	1.5	5.6
All			2.9	6.2

c) α-cyclodextrin glucosidic bond torsion angles

	Torsion angle		Fluctuation
	exp	MD	MD
C32–C42–O42–C11	+134.7	+127.0	8.2
C33–C43–O43–C12	+130.0	+123.2	7.8
C34–C44–O44–C13	+126.6	+120.6	7.4
C35–C45–O45–C14	+116.8	+113.8	8.4
C36–C46–O46–C15	+170.9	+158.5	9.8
C31–C41–O41–C16	+121.5	+113.5	7.7
All C3–C4–O4–C1	+133.4	+126.1	8.2

Glucose torsion angles (Table 6) involving O2, O3, O6 but not hydrogen atoms are reproduced within an average deviation of 4°, where deviations including the O2 and O3 atoms range from 2° to 4° and deviations for O6 atoms are 6° on average. The latter contain two major exceptions. One is O6 of the twisted glucose unit 5 with a difference of 12.9° between the MD and the experimental value. O65 makes a hydrogen bond to an internal water molecule OWA, whereas the other O6 atoms are connected to other water molecules or, intermolecularly, to hydroxyl-groups. The other exception is O61 which forms a strong (78.7%) intermolecular hydrogen bond to O63 of molecule 11 and a weak (2.2%) intramolecular bond to O65, which causes the large fluctuation of 29 degrees.

This fluctuation reflects the experimentally observed disorder of this group (the only one in the crystal structure), which is 92% occupied in O61A

Table 6. α-cyclodextrin glucose ring side-chain torsion angles (in degrees) in the 6 glucose units for the experimental structure and from the MD simulation ⟨*M*1–16; 5–15 ps⟩. The last column gives the rms dynamical fluctuations of the torsion angles as observed in the simulation

Glucose unit	O5–C1–C2–O2			C1–C2–C3–O3			C4–C5–C6–O6		
	Torsion angle		Fluctuation	Torsion angle		Fluctuation	Torsion angle		Fluctuation
	exp	MD	MD	exp	MD	MD	exp	MD	MD
1	+174.3	−179.5	7.8	−170.0	−167.6	7.2	−169.9	−163.5	29.1
2	+175.9	−177.1	6.3	−170.2	−171.3	7.1	+ 46.6	+ 50.4	8.7
3	−179.6	−175.1	6.5	−175.1	−177.7	8.0	+ 59.6	+ 54.7	10.7
4	−178.6	−177.0	8.2	−177.1	+178.1	7.2	+ 48.6	+ 47.8	9.5
5	−177.3	−175.5	9.1	−173.7	−174.2	8.0	−171.5	−158.6	13.6
6	−179.3	−179.2	7.5	−174.0	−176.2	10.8	+ 52.9	+ 47.8	9.0
All	+179.2	−177.3	7.6	−173.4	−174.8	8.1	+ 97.7	+ 99.8	15.2
Glucose unit	C1–C2–O2–H2			C2–C3–O3–H3			C5–C6–O6–H6		
	Torsion angle		Fluctuation	Torsion angle		Fluctuation	Torsion angle		Fluctuation
	exp	MD	MD	exp	MD	MD	exp	MD	MD
1	+ 84.8	+144.2	40.2	− 60.2	− 75.4	20.1	−110.5	−113.8	347.2
2	+100.1	+102.2	16.8	+160.9	+174.6	20.4	+ 78.8	+ 75.7	14.3
3	+138.6	+141.2	15.8	+172.7	−176.6	25.2	+ 74.2	+ 59.9	34.1
4	− 50.4	− 76.5	375.1	+168.7	+177.8	13.6	−145.7	−155.2	16.5
5	+153.8	+168.8	31.2	− 86.0	− 96.0	26.4	+ 99.1	+ 65.6	171.0
6	− 34.0	− 46.9	129.3	−106.7	− 70.8	47.5	−117.8	−116.7	33.2
All	+ 65.5	+127.2	163.5	−138.4	−131.1	27.7	+159.7	− 90.8	159.4

and 8% in O61B, positions which correspond to O5–C5–C6–O6 torsion angles in the ranges +gauche (O61A) and −gauche (O61B). The average fluctuation of the torsion angles with O6 is about 15°, that is twice the value of 7° to 8° for angles with O 2 and O 3.

The sinusoidal potentials of the C2–O2, C3–O3, C5–C6 side-chain torsion angles are defined with a threefold symmetry (Eq. (1) and Table 2) so that the rotational potential shows three barriers and three minima. For the torsion angle $C_4–C_5–C_6–O_6$ of glucose unit 1, 8 transitions from one to the other minimum were found during the period from 5 to 15 ps. This result agrees with the experimental finding that O61 is twofold disordered and forms several hydrogen bonds intermolecularly to O63, intramolecularly to O65, O56, and also to the external water W3 (see above and Table 7). The torsion angles involving atoms H_2, H_3 and H_6 show many 120° transitions: 166, 66 and 31 respectively for all 16 α-CD molecules. This means an average of 1.7, 0.7 and 0.3 transitions per torsion angle per 10 ps. The rotational freedom of these torsion angles is also demonstrated by their large fluctuations, which are 163.5°, 27.7° and 159.4° on average.

Very large fluctuations for the H_6 torsion angles in glucose units 1 and 5 are related to the occurrence of the twist of unit 5 which also allows for large fluctuations of H_2 and H_3 torsion angles in unit 6. The large fluctuation of the H_2 torsion angle in unit 4 suggests that this hydroxyl group is involved in several hydrogen bonds; it is bound to O35, to O54, and to a water WB. An overall impression can be obtained from Fig. 3.

Water molecules

Of the six water molecules in the asymmetric unit, the experimentally observed positions of W_1, W_2, W_4, WB are reproduced by the MD simulation within their experimental accuracy. Water molecules W_3 and WA, which show the largest positional fluctuations in the simulations, are shifted from their experimental positions by 0.11 to 0.12 nm, when averaged over the 16 asymmetric units.

Figure 4 displays the shifts of individual water molecules. All W_1, W_2, W_4 and WB waters in the 16 asymmetric units have positional differences less than 0.08 nm. The largest deviation for waters WA and W3 was about 0.2 nm, except for two asymmetric units where water W3 drifted away from its experimental position by 0.36 nm and 0.44 nm. These shifts in water positions might be associated with the formation of dynamically disordered O–(1/2H)...(1/2H)–O hydrogen bonds of the flip-flop type which are observed in the MD simulation (2.2 and 5.1% for O61...WA,

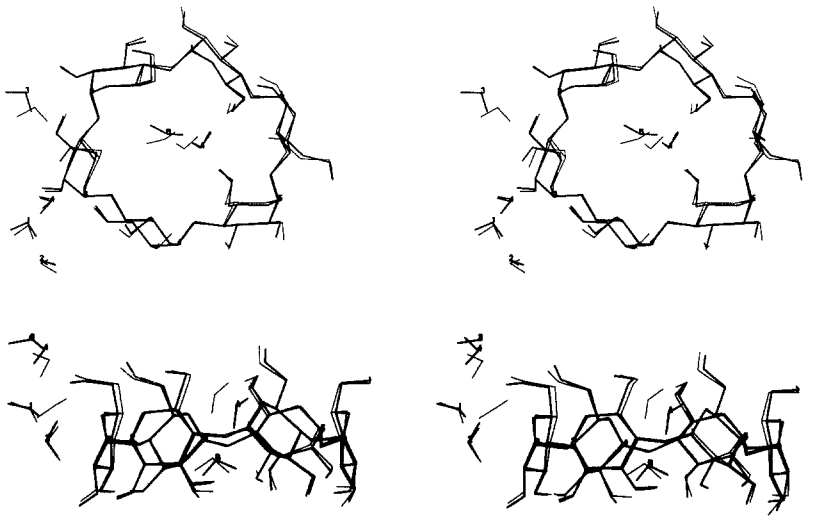

Fig. 3a and b. α-cyclodextrin + $6H_2O$ form I at 293 K. *Thin-lines:* neutron diffraction structure; *thick lines*. averaged MD structure

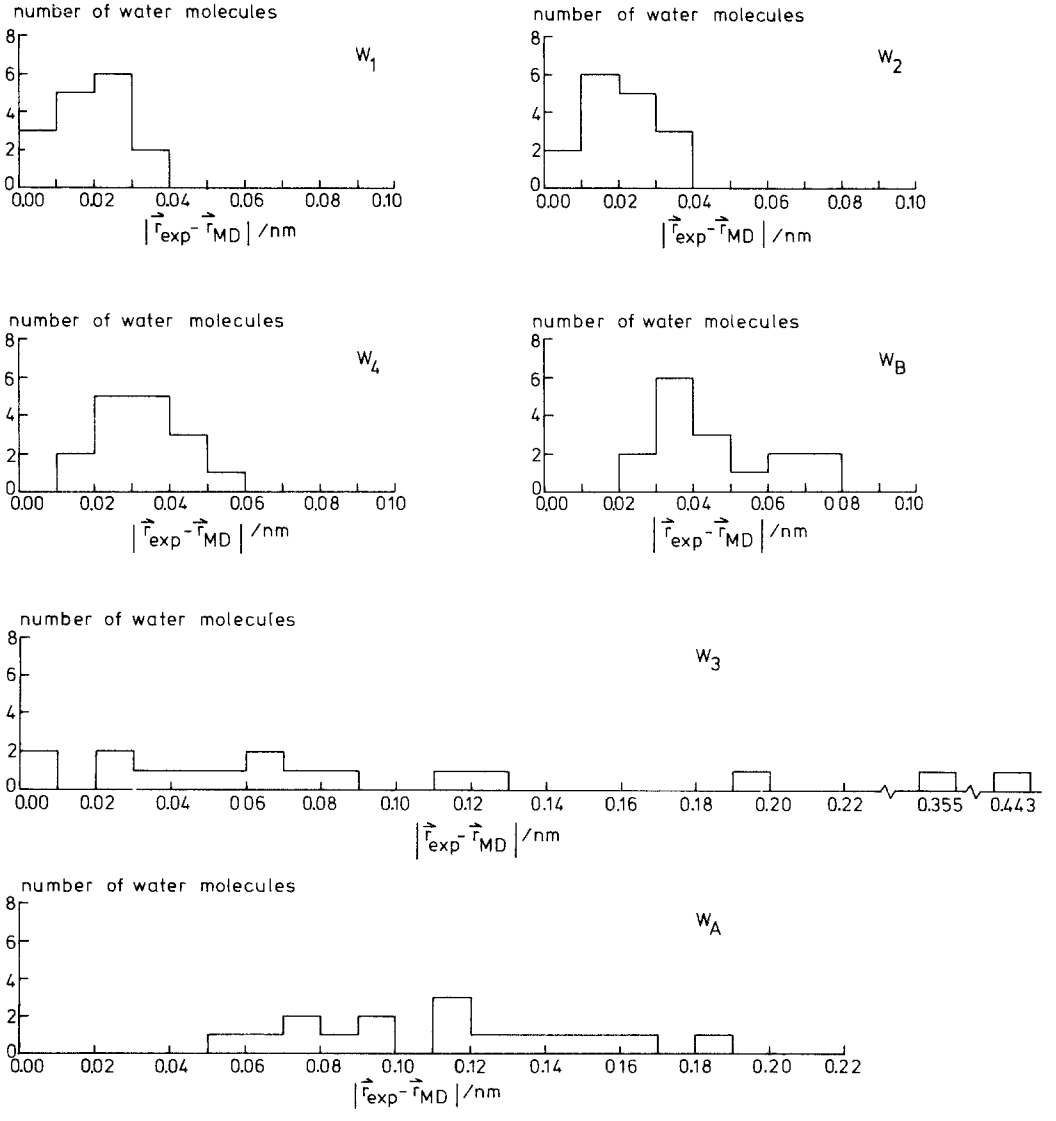

Fig. 4. Distribution of the positional rms difference (nm) between MD time-averaged and experimental water oxygen positions of the 6 independent water molecules in the 16 asymmetric units of the computational box

Table 7. Hydrogen bonds of α-cyclodextrin hexahydrate, form I, 293 K. The donor-acceptor (D-A) and the hydrogen-acceptor (H ... A) distances (in nm) for the hydrogen bonds and their angles D-H-A (in degrees). From the MD simulation ⟨*M*1–16; 5–15 ps⟩ hydrogen bonds with H ... A distances less than 0.25 nm and D-H-A angles larger than 135° were selected and their percentage of existence during the time period of 5–15 ps is given. Comparable experimental data are presented in the last three columns. The MD data were averaged over the 16 asymmetric units. It is denoted to which asymmetric unit an acceptor atom belongs, assuming that the donor atom belongs to unit 1

Symmetry code	Donor		Acceptor	MD				Experimental (ND)		
				%	D-A (nm)	H ... A (nm)	DHA (deg.)	D-A (nm)	H ... A (nm)	DHA (deg.)
a) Glucose → glucose, > 2%										
9	O31	H31	O65	96.4	0.267	0.171	162.3	0.261	0.167	158
7	O62	H62	O31	95.1	0.272	0.178	158.2	0.278	0.189	171
1	O32	H32	O21	91.5	0.285	0.189	160.4	0.295	0.209	175
1	O33	H33	O22	88.9	0.295	0.199	161.8	0.302	0.193	171
1	O34	H34	O23	88.6	0.284	0.192	153.1	0.282	0.186	161
14	O35	H35	O64	80.3	0.266	0.170	161.3	0.272	0.177	169
11	O61	H61	O63	78.7	0.279	0.184	159.8	0.281	0.177	177
14	O36	H36	O34	72.3	0.275	0.181	158.8	0.279	0.189	163
9	O64	H64	O22	69.7	0.280	0.189	151.9	0.285	0.195	160
6	O25	H25	O33	59.3	0.286	0.192	158.8	0.290	0.195	169
5	O63	H63	O66	42.9	0.272	0.177	159.6			
1	O26	H26	O31	38.9	0.297	0.204	156.5	0.302	0.214	150
14	O24	H24	O54	35.5	0.302	0.209	156.4			
14	O25	H25	O64	31.3	0.291	0.197	158.8			
9	O64	H64	O32	27.4	0.296	0.207	147.1			
9	O21	H21	O61	13.9	0.306	0.214	155.5			
5	O36	H36	O33	12.3	0.286	0.190	160.8			
14	O26	H26	O34	10.8	0.299	0.210	150.2			
9	O21	H21	O65	9.6	0.294	0.204	152.1			
5	O66	H66	O63	5.0	0.297	0.210	147.8			
1	O35	H35	O24	5.0	0.316	0.223	156.5			
1	O24	H24	O35	3.5	0.316	0.225	151.1	0.337	0.285	118
14	O33	H33	O25	3.3	0.313	0.221	153.2			
15	O63	H63	O61	3.1	0.284	0.189	160.7			
1	O61	H61	O65	2.2	0.304	0.210	157.6			
1	O31	H31	O26	2.0	0.298	0.204	160.6			
b) Glucose → water, > 2%										
10	O23	H23	OW2	98.1	0.273	0.176	163.1	0.272	0.185	179
9	O22	H22	OW4	98.1	0.269	0.173	162.4	0.269	0.177	169
5	O66	H66	OW1	93.0	0.271	0.174	164.1	0.290	0.197	169
1	O65	H65	OWA	91.3	0.271	0.174	163.8	0.277	0.192	176
3	O21	H21	OW3	65.3	0.274	0.178	161.3	0.281	0.176	166
1	O63	H63	OW4	48.1	0.279	0.185	159.2	0.289	0.187	166
6	O24	H24	OWB	18.9	0.295	0.200	160.6			
1	O65	H65	OWB	5.8	0.271	0.174	163.5			
13	O26	H26	OW1	5.7	0.270	0.173	164.5			
11	O61	H61	OW3	5.6	0.304	0.217	145.9			
3	O32	H32	OW3	4.8	0.296	0.204	155.8			
6	O35	H35	OWB	2.5	0.296	0.207	149.3			
1	O61	H61	OWA	2.2	0.208	0.301	155.7			
c) Water → glucose, > 2%										
6	OW2	HW1	O25	98.8	0.276	0.179	163.0	0.272	0.175	174
6	OW2	HW2	O36	95.2	0.276	0.181	158.8	0.277	0.175	169
13	OW1	HW2	O26	82.6	0.282	0.188	158.5	0.275	0.186	152
15	OW4	HW1	O62	55.3	0.287	0.194	157.1	0.284	0.198	169
1	OW3	HW1	O63	50.9	0.289	0.195	157.6	0.283	0.193	171
5	OW3	HW2	O56	41.3	0.301	0.208	156.5			
1	OWA	HW1	O61	36.4	0.297	0.204	156.5	0.297	0.198	173
15	OW4	HW2	O62	31.6	0.287	0.194	155.4			
14	OWB	HW2	O35	27.0	0.291	0.198	154.6			
14	OWB	HW2	O24	21.9	0.295	0.204	154.0	0.299	0.205	160

Table 7 (continued)

Symmetry code	Donor	Acceptor	MD				Experimental (ND)		
			%	D-A (nm)	H...A (nm)	DHA (deg.)	D-A (nm)	H...A (nm)	DHA (deg.)
c) Water → glucose, > 2%									
14	OWB HW1	O35	19.5	0.292	0.201	153.0	0.311	0.227	145
1	OW3 HW2	O63	13.3	0.290	0.198	153.3			
14	OWB HW1	O24	13.1	0.299	0.207	154.5			
15	OW3 HW2	O61	11.4	0.304	0.213	152.8	0.333	0.285	107[a]
1	OWA HW1	O41	9.3	0.311	0.220	152.5			
7	OW3 HW1	O21	8.7	0.295	0.203	153.9			
15	OW3 HW1	O61	8.3	0.307	0.216	152.6			
5	OW3 HW1	O56	7.3	0.304	0.213	152.2			
1	OWB HW1	O44	7.3	0.306	0.214	154.6			
13	OW1 HW1	O26	5.7	0.284	0.190	157.7			
1	OWA HW2	O61	5.1	0.301	0.209	154.2			
5	OW1 HW2	O66	4.9	0.286	0.193	155.7			
1	OWB HW2	O43	4.3	0.311	0.221	152.4			
1	OWB HW2	O44	4.3	0.311	0.220	152.9			
1	OWB HW1	O43	4.2	0.311	0.220	152.4			
15	OW4 HW2	O51	3.4	0.297	0.207	150.5			
1	OWB HW1	O42	3.3	0.307	0.216	151.7			
5	OW4 HW1	O66	2.8	0.312	0.224	147.7			
15	OW4 HW1	O51	2.8	0.303	0.214	148.9			
5	OW3 HW2	O66	2.7	0.314	0.227	145.9	0.334	0.272	117
14	OWA HW1	O24	2.5	0.305	0.216	148.4			
1	OW4 HW2	O63	2.5	0.304	0.212	154.1			
1	OWB HW1	O61	2.3	0.294	0.201	156.0			
14	OWA HW2	O24	2.3	0.312	0.223	150.4			
14	OWA HW2	O35	2.0	0.289	0.196	156.0			
d) Water → water, >1%									
1	OW1 HW1	OW2	90.6	0.288	0.191	163.2	0.286	0.184	176
1	OWA HW2	OWB	70.1	0.284	0.188	161.2	0.292	0.204	167
1	OW4 HW2	OW1	50.1	0.291	0.196	161.3	0.287	0.187	171
1	OW4 HW1	OW1	27.3	0.294	0.199	161.1			
1	OWA HW1	OWB	10.5	0.292	0.199	156.4			
1	OWB HW2	OWA	7.4	0.292	0.202	150.7			
1	OW1 HW2	OW2	5.9	0.290	0.194	162.1			
11	OWA HW1	OW3	4.4	0.293	0.201	153.5			
11	OWB HW1	OW3	3.5	0.290	0.198	153.8			
15	OW3 HW1	OWA	3.2	0.304	0.214	150.3			
1	OWB HW1	OWA	2.7	0.295	0.206	148.4			
15	OW3 HW2	OWA	1.5	0.300	0.208	154.2			

[a] Not given in (Klar et al. 1980) due to poor geometry

see Table 7b,c and 70.1, 10.5, 7.4 and 2.7% for WA...WB, see Table 7d).

Averaged over all water molecules, the difference between experimental and MD water positions of 0.072 nm is larger than that for the α-CD atoms, which is 0.025 nm. A corresponding observation can be made for the overall atomic fluctuations; the water molecules display a value of 0.070 nm (exp. 0.047 nm) and the α-CD atoms a value of 0.049 nm (exp. 0.036 nm). Because of the higher mobility of water molecules which is associated with their weak binding by hydrogen bonds, it is not surprising that their average positions are less well reproduced in the simulation.

One may compare the results obtained here with those of previous MD studies (Mezei et al. 1983; Vovelle et al. 1985). Mezei et al. (1983) distinguish three types of agreement: if in all asymmetric units the deviation between experiment and simulation is smaller than 0.06 nm, there is *full* agreement; if this is only true in at least one asymmetric unit, it is called *partial* agreement; if none of these cases is true, it is called no agreement. In the deoxycytidylyl-3′,5′-guanosine/proflavin crystal, the following is found: full agreement 5 positions; partial agreement 11 positions; no agreement 11 positions. When applying the same criterion to our α-CD simulation, we find full agree-

ment for 3 sites (W_1, W_2, W_4) and partial agreement for the other three sites.

In the MD study on the vitamin B_{12} crystal structure the rms deviation between simulated and experimental water positions ranged from 0.075 nm to 0.126 nm for various force fields (Vovelle et al. 1985). The value of 0.072 nm found here for the α-CD hexahydrate crystal is lower. One might expect better agreement in the α-CD case, because the α-CD crystal contains fewer water sites per asymmetric unit. However, in the α-CD MD simulation *all* the atoms, including those of the cyclodextrin, were allowed to move, whereas in the deoxycytidylyl-3′,5′-guanosine/proflavin and vitamin B_{12} studies only the water molecules could move. They were more or less positionally restrained by the rigidity of the solutes. Therefore, compared to previous studies the reproduction of the water sites in the crystal lattice of α-CD · $6H_2O$ is quite satisfactory.

Hydrogen bonds

The neutron diffraction structure and the averaged MD structure ⟨*M*1–16; 5–15 ps⟩ have a similar hydrogen bond network, see Table 7 and Figs. 5 and 6. The hydrogen bond criterion that is applied to the MD trajectory is: distance (H ... A) < 0.25 nm and angle (D–H ... A) > 135°.

The most important result is that hydrogen bonds, which have a high occurrency in the MD trajectory, have also been located experimentally. Bonds with lower populations, which exist only for shorter periods, are not described in the experimental paper. This is because diffraction methods display the most stable configuration of a crystal structure, and populations of atoms below 20% are not seen. On the other hand molecular dynamics shows a variety of structures which the molecule can adopt during the simulation period and gives a quantitative estimate for their percentage of occurrence [1]. Let us look more closely at some details.

a) The five intramolecular hydrogen bonds between O2 and O3 hydroxyl groups of adjacent glucose units within the same α-CD molecule are reproduced as well as the fact that there is no O25 ... O36 interaction. The O24–H24 ... O35 bond has an unusual experimental geometry and does not satisfy the hydrogen bond criterion applied here. In agreement, the MD simulation yields a much lower occurrence (percentage in Table 7a) than for the other four hydrogen bonds of that type. Also its orientation can be reversed in flip-flop mode to O35–H35 ... O24. This reversion is also seen in MD for the pair of hydrogen bonds O26–H26 ... O31 and O31–H31 ... O26 [2].

b) All seven intermolecular glucose–glucose hydrogen bonds are reproduced with the highest percentage in MD. There are 11 additional bonds in MD with occurrency > 3%.

c) The six glucose → water hydrogen bonds exist in both experimental and MD data, see Table 7b. In MD there are some more such interactions with lower per-

1 A more detailed analysis of this subject will be given in our following paper about flip-flop hydrogen bonding

2 See Footnote [1]

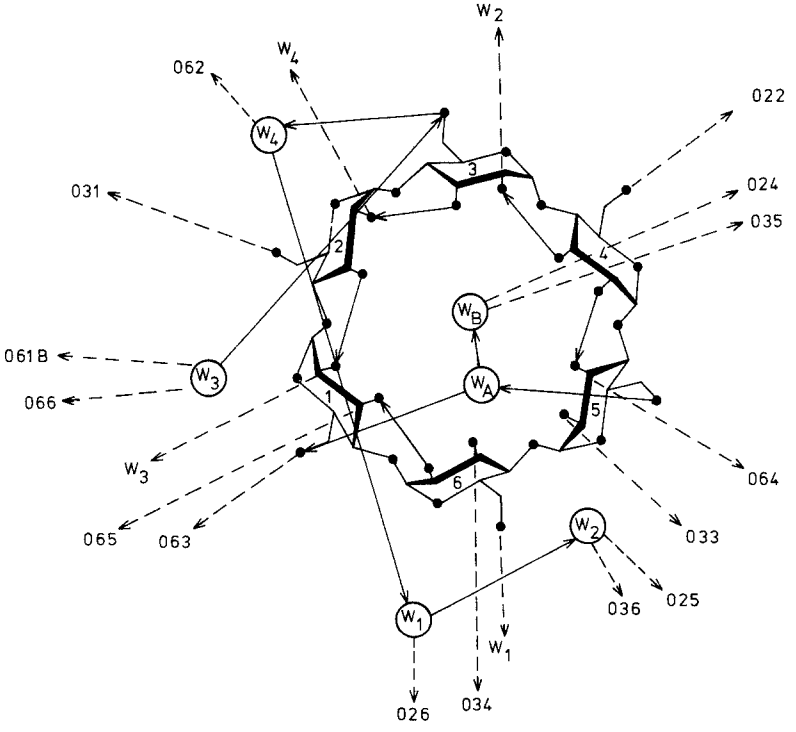

Fig. 5. Hydrogen bonds of α-cyclodextrin · $6H_2O$, form I, at 293 K, neutron diffraction structure. *Dashed* and *solid lines* indicate hydrogen bonds, their *arrow* points towards the acceptor atom, *double arrows* display hydrogen bonds existing in both directions

centages, for example O24–H24 ... OWB with about 19%.

d) Concerning the water → glucose hydrogen bonds given in Table 7c, the highest occupied MD interactions are also seen in the neutron diffraction analysis. There are several hydrogen bonds in the 27% to 41% population range which were not observed experimentally, as are several of the hydrogen bonds between WA, WB and the O4 atoms, which, however, are only present in the <10% range. In general, the experimental water → glucose hydrogen bonds are simulated by MD, but not all of them are of highest population. MD predicts an OW3–HW2 ... O56 bond with 41% occurrency, which also might explain the MD shift of water W3; the OW3–HW2 ... O66 bond with poor experimental geometry has a low occurrency of 2.7%. Neutron diffraction distinguishes between an O61A site with 92% occupancy and an O61B site with only 8% (Klar et al. 1980). Our MD simulation was carried out with the O61A coordinates. The experimental OW3–HW2 ... O61 bond leads to the B site, in MD it prefers the A site with an occurrency of 11.4%, and the O61B site is not reproduced.

e) The three strongest water → water hydrogen bonds in the MD study represent the corresponding experimentally detected interactions. Table 7d suggests that besides the experimental WA–H ... WB interaction, in the MD simulation the two included water molecules WA and WB form all kinds of possible hydrogen bonds with each other, although at low occurrency < 10.5%, including interactions of the disordered flip-flop type, O–(1/2H) ... (1/2H)–O.

Conclusions

The neutron diffraction structure of α-CD · $6H_2O$, form I and the averaged Molecular Dynamics structure ⟨*M* 1–16; 5–15 ps⟩ for 16 α-CD + $96H_2O$ molecules simulated for a period of 15 ps at $T = 293$ K are very similar. The α-CD atoms have on average only been displaced by about 0.025 nm, four waters by about 0.03 nm, and water W3 and water WA by 0.12 nm. Fluctuations calculated from experimental B-values and from the MD simulation agree in most cases.

The average of the root mean square positional differences between experimental and MD structures is less than or of the order of the experimentally obtained rms fluctuations (0.03 nm ring-atoms, 0.04 nm side-chains), and for the water molecules it is about 0.07 nm. The main characteristics are well reproduced like the twisted glucose unit 5 with a glucosidic bond torsion angle of about 158° (exp. 170°) instead of 120° and the hydrogen bond from O65 to the included water WA with occurrency of 91%. The five intramolecular hydrogen bonds between O2 and O3 hydroxyl groups of adjacent glucose units and the large O25 ... O36 distance observed experimentally are also found in the MD simulation, i.e. the α-CD molecule has the tendency to remain in the "collapsed" form typical for the water inclusion complex and does not prefer the "round, relaxed" structure observed in inclusion complexes with guest molecules other than water. This is in agreement with earlier suggestions concerning the mechanism of inclusion formation (Saenger 1980).

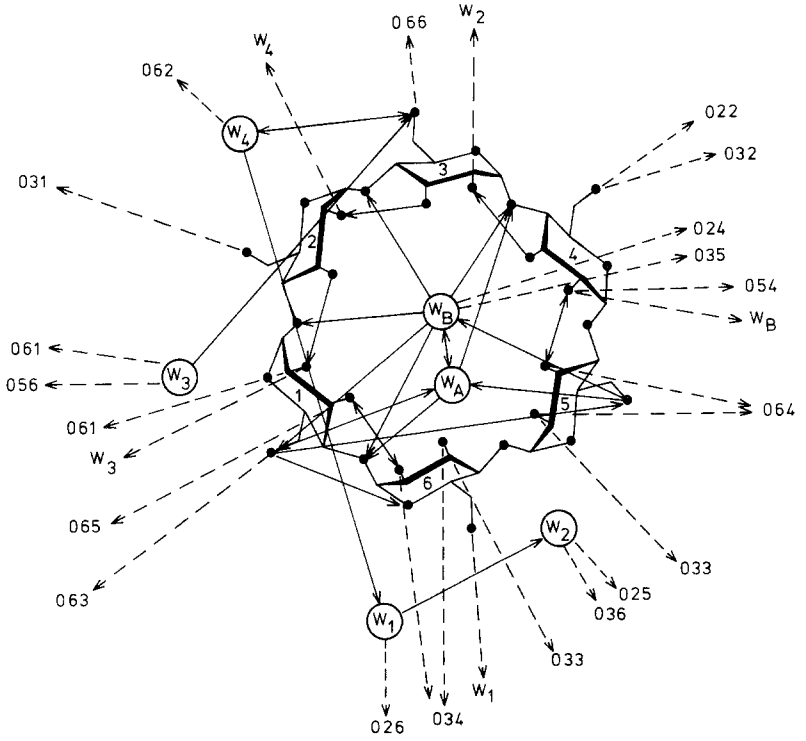

Fig. 6. Hydrogen bonds of α-cyclodextrin · $6H_2O$, form I, at 293 K, molecular dynamics simulation, ⟨*M* 1–16; 5–15 ps⟩

Atoms with multiple sites like O61A and O61B as obtained from neutron diffraction refinement show large MD-fluctuations, which means, that the crystallographic disorder phenomenon is explained by a high mobility of the corresponding atom in the MD simulation.

In general, hydrogen bonds with occurrency above 50% in the MD study are also observed experimentally. A striking example where all geometrically possible hydrogen bonds between two water molecules are present in the MD simulation, is found with the two included waters WA and WB. They interact also with glucose O4 oxygen atoms at a low percentage ($< 10\%$), which, if really occurring, could not be seen experimentally.

Finally, we conclude that the experimental properties of the α-CD $\cdot$ $6H_2O$ crystal are well reproduced by the force field that is used in the MD simulation presented here. It could well be that the experimental data obtained with "hedgehog", a 100-counter-diffractometer, are not good enough to really provide for a reliable basis for this MD study because the reliability factor for the refinement was only 11%. Therefore, new neutron diffraction data have to be collected in order to find out whether the hydrogen bonds simulated with lower occupancy really have a physical meaning.

Acknowledgements. We thank H. J. C. Berendsen for simulating discussions and H. T. Jonkman for continuing support concerning our calculations on the VAX-computer of the Department of Chemistry of the University of Groningen. This work was supported by a grant to J.E.H.K. (Nachwuchsförderung) of the Land Berlin and by the German Federal Minister for Research and Technology (BMFT) under the contract number FKZ: O3B72AO79.

References

Åqvist A, Gunsteren WF van, Leijonmarck M, Tapia O (1985) A molecular dynamics study of the *c*-terminal fragment of the L7/L12 ribosomal protein. Secondary structure motion in a 150 ps trajectory. J Mol Biol 183:461–477

Berendsen HJC, Gunsteren WF van (1984) Molecular dynamics simulations: techniques and approaches. In: Barnes AJ, Orville-Thomas WJ, Yarwood J (eds) NATO ASI Series, vol C135. On molecular liquids – dynamics and interactions. Reidel, Dordrecht, pp 475–500

Berendsen HJC, Postma JPM, Gunsteren WF van, Hermans J (1981) Interaction models for water in relation to protein hydration. In: Pullman B (ed) Intermolecular forces. Reidel, Dordrecht, pp 331–342

Berendsen HJC, Postma JPM, Gunsteren WF van, di Nola A, Haak JR (1984) Molecular dynamics with coupling to an external bath. J Chem Phys 81:3684–3690

Berendsen HJC, Gunsteren WF van, Zwinderman HRJ, Geurtsen RG (1986) Simulations of proteins in water. Ann NY Acad Sci (in press)

Chacko KK, Saenger W (1981) Topography of cyclodextrin inclusion complexes. 15. Crystal and molecular structure of the cyclohexaamylose – 7.57 water complex, form III. Four and six-membered circular hydrogen bonds. J Am Chem Soc 103:1708–1714

Cramer F, Saenger W, Spatz HC (1967) Inclusion compounds, XIX. The formation of inclusion compounds of α-cyclodextrin in aqueous solutions. Thermodynamics and kinetics. J Am Chem Soc 89:14–20

Gunsteren WF van, Berendsen HJC (1977) Algorithms for macromolecular dynamics and constrained dynamics. Mol Phys 34:1311–1327

Gunsteren WF van, Berendsen HJC (1985) Molecular dynamics simulations: techniques and applications to proteins. In: Hermans J (ed) Molecular dynamics and protein structure. Polycrystal Books Service, Western Springs, Ill, pp 5–14

Gunsteren WF van, Karplus M (1982) Effect of constraints on the dynamics of macromolecules. Macromolecules 15:1528–1544

Gunsteren WF van, Berendsen HJC, Hermans J, Hol WGJ, Postma JPM (1983) Computer simulation of the dynamics of hydrated protein crystals and its comparison with X-ray data. Proc Natl Acad Sci USA 80:4315–4319

Hingerty B, Klar B, Hardgrove GL, Betzel C, Saenger W (1984) Neutron diffraction of alpha, beta and gamma cyclodextrins: hydrogen bonding patterns. J Biomol Struct Dyn 2:249–260

Kim KS, Clementi E (1985) Hydration analysis of the intercalated complex of deoxydinucleoside phosphate and proflavin; computer simulations. J Phys Chem 89:3655–3663

Klar B, Hingerty B, Saenger W (1980) Topography of cyclodextrin inclusion complexes. XII. Hydrogen bonding in the crystal structure of α-cyclodextrin hexahydrate: the use of a multicounter detector in neutron diffraction. Acta Crystallogr B36:1154–1165

Krüger P, Strassburger W, Wollmer A, van Gunsteren WF (1985) A comparison of the structure and dynamics of avian pancreatic polypeptide hormone in solution and in the crystal. Eur Biophys J 13:77–88

Kuriyan J, Petsko GA, Levy RM, Karplus M (1986) Effect of anisotropy and anharmonicity on protein crystallographic refinement. An evaluation by molecular dynamics. J Mol Biol 190:227–254

Lindner K, Saenger W (1982) Topography of cyclodextrin inclusion complexes. XVI. Cyclic system of hydrogen bonds: structure of α-cyclodextrin hexahydrate, form (II): comparison with form (I). Acta Crystallogr B38:203–210

Manor PC, Saenger W (1974) Topography of cyclodextrin inclusion complexes. III. Crystal and molecular structure of cyclohexaamylose hexahydrate, the (H_2O_2) inclusion complex. J Am Chem Soc 96:3630–3639

Mezei M, Beveridge DL, Berman HM, Goodfellow JM, Finney JL, Neidle S (1983) Monte Carlo studies on water in the dCpG/proflavin crystal hydrate. J Biomol Struct Dyn 1:287–297

Ryckaert JP, Ciccotti G, Berendsen HJC (1977) Numerical integration of the cartesian equations of motion of a system with constraints: molecular dynamics of *n*-alkanes. J Comput Phys 23:327–341

Saenger W (1980) Cyclodextrin inclusion compounds in research and industry. Angew Chem (Int Ed Engl) 19:344–362

Saenger W, Betzel C, Hingerty B, Brown GM (1982) Flip-flop hydrogen bonding in a partially disordered system. Nature 296:581–583

Vovelle F, Goodfellow JM, Savage HFJ, Barnes P, Finney JL (1985) Solvent structure in vitamin B_{12} coenzyme crystals. Eur Biophys J 11:225–237